A HIGH PERFORMANCE AUXILIARY POWER UNIT FOR A SERIES HYBRID ELECTRIC VEHICLE

FINAL REPORT

NOVEMBER 2000

Report Budget Number KLK331

Report N01-22

Prepared for

OFFICE OF UNIVERSITY RESEARCH AND EDUCATION

U.S. DEPARTMENT OF TRANSPORTATION

Prepared by

NATIONAL INSTITUTE FOR ADVANCED TRANSPORTATION TECHNOLOGY

UNIVERSITY OF IDAHO

Dean Edwards, PhD PE

James Richards, MSME

TABLE OF CONTENTS

EXECUTIVE SUMMARY

The objective of this work was to investigate small, high-speed, gasoline engines for use in a series hybrid electric vehicle (HEV). A high performance auxiliary power unit (HPAPU) that consists of a small, high-speed engine directly coupled to an alternator was designed to provide enough power for steady state operation. A dynamic engine model was developed to characterize the performance of engines used in this design for control system development.

The engine model was based on previously developed heat release engine models but tailored for control system development by operating in the time domain and having a short computation time. To determine the required power output of a high performance APU in a series HEV, a steady state road load analysis program was developed using Matlab.

One conclusion of this work was that a high performance APU weighing less than 41 kg (90 lbs.) and occupying a volume less than .09 cubic meters (3 cubic feet) can provide enough power for a 1800 kg (4000 lbs.) series HEV to operate at freeway speeds. A Yamaha 250cc, four-stroke, SI engine is the best commercially available engine for this application. The engine model was validated against its specifications.

DESCRIPTION OF PROBLEM

It is becoming obvious that the current rate of energy consumption by automobiles will not be sustainable indefinitely, and the present rate of pollution formation is changing the Earth's environment. One way of reducing the energy consumed by automobiles is to use more energy-efficient propulsion systems. Current technology has been applied to create more energy efficient vehicle propulsion systems by combining an internal combustion (IC) engine and an electric propulsion system into a single system that is more efficient than conventional vehicles using an IC engine alone. A vehicle that combines an IC engine and an electric propulsion system is commonly called a Hybrid Electric Vehicle (HEV).

Series HEVs only have an electric propulsion system coupled to the wheels. Power for the electric propulsion system comes from the battery pack and or the auxiliary power unit (APU). The APU generates electrical power that is used by the electric propulsion system during extended range operation. For short-range operation, which is typical of most daily driving conditions, a series HEV can be completely powered by the battery pack and operate as a zero tailpipe emission vehicle (ZEV). Typically, the energy for recharging the battery pack comes from electricity supplied by the grid.

The greatest advantage of a series HEV vehicle is achieving reduced emissions and improved fuel economy by using grid electricity as a source of energy instead of burning fuel in the APU. Series HEV emissions are improved over conventional automobiles because monitoring and reducing pollutant formation at centralized points of electric power generation is easier and more cost effective than attempting the same with many automobiles using IC engines. The use of stored grid electricity to power series HEVs also moves the point of pollution formation to where grid power is generated and away from population centers that experience the worse air pollution.

The emissions created by operating the series HEV will also be reduced because the efficiency of producing grid electricity and storing it in the vehicle's battery pack can be more efficient

than operating an internal combustion APU. Modern power generation facilities are around 70 percent efficient at converting fossil fuels into electrical power [4]. Assuming a battery charging efficiency of 90 percent and a propulsion system efficiency of 90 percent, a series HEV could be as high as 58 percent efficient at converting grid electricity to vehicle motion. The best performing diesel engines available today, under ideal operating conditions, are at most 45 percent efficient at converting fossil fuels to vehicle motion [5]. Spark ignition (SI) engines are even less efficient than diesel engines. The operating efficiency of series HEVs will be increased as more efficient power plants are built, such as hybrid cycle natural gas power plants, and with the development of alternative energy sources like nuclear and solar power.

If a series HEV could store enough energy from the grid to power the vehicle for 60 miles, most daily driving situations could be met with zero tailpipe emissions. This statement is based on a 1995 survey of vehicle usage in the United States that reported the average distance traveled by a vehicle was 32.15 miles per day [1] and over 80 percent of vehicles did not drive more than 60 miles per day [2, 3]. However, due to the size of the components that make up a series HEV system, electric propulsion system, APU, and battery pack, it is difficult to package the system in a mid-size vehicle chassis without reducing the passenger and cargo space or detrimentally affecting acceleration performance. This work presents an APU concept for a series HEV that reduces the size and weight of the APU while meeting the power demands for highway driving.

The APU concept presented in this report is called a high performance APU (HPAPU). The small size and weight of the HPAPU allows a series HEV system to have a 60 mile zero tailpipe emission range and fit into a mid-size automobile chassis while maintaining the long range capability of the series HEV. In addition, passenger space, cargo space, and vehicle performance are not sacrificed. Having enough electric energy storage in the batteries for 60 miles of operation as an electric vehicle means that most daily driving situations can be met using energy from the grid and not from the APU.

APPROACH AND METHODOLOGY

The objective of this work was to investigate small, high-speed gasoline engines for use in a series HEV. Our approach was to develop a series HEV design that uses a high performance, auxiliary power unit (HPAPU). In order to accomplish this design, we created a dynamic engine model that could be used in future development of HPAPU control systems. In the process of designing the series HEV, a steady state road load model was developed using Matlab. This steady state road load model was used to help size the battery pack based on vehicle specifications, determine the required power output of the APU and estimate the steady state fuel economy of the series HEV while the HPAPU is running. The engine model is validated against a single power/speed point of a four-stroke, 250cc Yamaha motorcycle engine, and closed loop speed control is implemented in the engine model and simulated under step and ramp disturbances.

FINDINGS; CONCLUSIONS; RECOMMENDATIONS

The findings are divided into two sections. In the first section a design for a series HEV is presented. Based on the design, the power requirement for the APU is established and components selected. In the second section, a dynamic engine model is developed and some control strategies investigated. The conclusions are discussed in the third section.

1.0 Series HEV Design

A series HEV design that includes a HPAPU is presented in this section. The series HEV design specifies a chassis and drivetrain, determines the required battery pack size and specifies the components for a HPAPU. This series HEV design will have all of the passenger space and creature comforts of a 2001 Ford Taurus with the additional feature that it will be able to run as a ZEV and use electrical energy from the grid to recharge the battery pack. For everyday driving, an electric propulsion system and lead-acid battery pack will power the vehicle. For extended range operation, a HPAPU will be used to provide power to the electric propulsion system.

The series HEV design presented in this thesis will operate as a zero tailpipe emission vehicle (ZEV) for everyday driving, while retaining the ability to drive long ranges. The range and speed requirements of this series HEV design are for 60 miles at 55 mph of zero tailpipe emission operation. A zero tailpipe emission range of 60 miles will allow this vehicle to gain the efficiency and emission advantages of using grid electricity by operating as a ZEV for approximately 80 percent of the time.

A steady state road load analysis program that was developed to aid in designing the series HEV is also presented in this chapter. The steady state road load program was written using Matlab and performs the functions of sizing a battery pack based on the vehicle specifications, determining the required power output of the APU and estimating the steady state fuel economy of the vehicle while the APU is running. A parametric study was conducted on the

battery pack specific energy to assess the affects on the weight and volume of the battery pack, vehicle performance, and the HPAPU power requirement.

1.1 Vehicle Design

The focus of this series HEV vehicle design is on the HPAPU. Before the components of the HPAPU can be specified, the required power output of the HPAPU must be known. To determine the required HPAPU power output the weight, frontal area, drag coefficient, and rolling resistance coefficient must be known or estimated for the vehicle that the HPAPU is powering. First the weight of the vehicle without the battery pack is determined by making an assumption for the weight of the HPAPU. Then the road load model is used to specify the size of the battery pack, find the total vehicle weight, and determine the steady state power requirements of the series HEV.

1.1.1 Chassis

This series HEV design is based on the specifications for a 2001 Ford Taurus (Table 1.1) [6]. The reason for choosing the Ford Taurus as the platform for this design is that the Taurus is one of the most popular four-door sedans on the U.S. market and has the performance level and creature comforts that consumers are accustomed to and expect in a new vehicle. To be widely accepted, a series HEV must have the same creature comforts and performance and be comparable in cost.

Table 1.1 Stock 2001 Ford Taurus Specifications

Body Type	Sedan
Drive train	Front engine, front drive
Airbag	Driver/passenger/sid
Base curb weight, lb.	3340
Base engine	3.0 liber V-6, OHV, 153 hp
Price range	$18,000—$23,000
Fuel economy, city/hwy	21/30 mpg, city/highway

1.1.2 Drivetrain

An electric propulsion system having an AC induction motor can provide the required power for a mid-size automobile in a small, lightweight package. For this design, the specifications

for an AC Propulsion 150kW system are used (Table 2.2) [7]. This system weighs 180 pounds not including the battery pack, and is about 180 pounds lighter than the 3.0L V6 IC engine that comes stock in the Ford Taurus.

Table 1.2 AC Propulsion 150 kW System Specifications

AC Propulsion 150 kW Propulsion System	
Voltage	336 VDC nominal
Current	520 A maximum
Torque	165 ft-lb maximum
Power	200 hp max, 70 hp continuous
Efficiency	91 percent peak (40 hp, 8500 rpm)
	86 percent road load (10 hp, 8500 rpm)
	>90 percent recharge (240V line, 10 kW)
Charger	Operates on 100-250 VAC
	20kW maximum power
Weight	110 lb. Motor
	70 lb. Controller w/ integral charger

The weight of this series HEV design is estimated to be 500 to 800 pounds, or 15 to 25 percent heavier than the stock Ford Taurus. Acceleration performance will be maintained with the additional weight by replacing the 114 kW 3.0L V6 internal combustion engine with the 150 kW AC Propulsion system. This is a 30 percent increase in maximum power output. This series HEV design can potentially have better acceleration performance than the Ford Taurus because the power increase is larger than the weight increase from the Ford Taurus platform.

1.1.3 Vehicle Weight

The overall vehicle weight is based on the specifications of a Ford Taurus (Table 1.1). The curb weight of a 2001 Ford Taurus is 3340 pounds. The IC engine is assumed to weigh approximately 360 pounds. Subtracting the engine weight from the curb weight results in a vehicle shell weight of 2990 pounds. The shell weight includes all of the vehicle components except the engine. After the weight of the HPAPU and electric propulsion system are added to the shell weight of the vehicle, the weight of this series HEV design, without the weight of the battery pack, is found to be 3260 pounds. The weight of the HPAPU was initially estimated to be around 100 pounds, and this weight was used in the series HEV design. The weight estimate for the HPAPU turned out to be fairly accurate, as will be seen later in this chapter.

Table 1.3 Vehicle Weight (lbs.) without Battery Pack

Ford Taurus Base Curb Weight	3340
3.0L V6 Engine Removed	-360
AC Electric Motor	110
AC Power Electronics	70
High Performance APU	100
	3260

1.1.4 Battery Pack

Energy storage in batteries presents the most difficult problem in designing a series HEV. The specific energy capacity of batteries is such that the size and weight of the battery pack are the factors that limit the electric only range of a series HEV. The range specification of 60 miles is too short to make an all-electric vehicle appealing to a consumer who is accustomed to the range and availability of conventional automobiles. This is the reason for including a HPAPU in this vehicle system. The short-range advantages of an electric vehicle can be realized while not sacrificing long-range driving capability.

The weight of a series HEV is dependent upon the weight of the battery pack. The size and weight of the battery pack is dependent upon the speed and range requirements of the vehicle and the energy capacity of the battery pack. Equation 1.1 shows the relationship of the zero tailpipe emission speed and range requirements on the weight of the battery pack. As the zero tailpipe range is increased, the mass of the battery pack increases. It may appear that the mass of the battery pack is reduced as the velocity requirement is increased because it is in the denominator of Eq. 1.1. However, as the required velocity is increased the required power increases proportional to the square of the velocity. This relationship can be seen in the road load equation (Eq. 1.2 [5]), where P_r and the required power are the same term.

$$mass_{batt} = \frac{range \times req.\ power}{specific\ energy \times velocity} \tag{1.1}$$

$$P_r(hp) = \frac{[C_R \cdot W_V + 0.0025 \cdot CD \cdot A_F \cdot V_{MPH}]V_{MPH}}{375} \tag{1.2}$$

The HPAPU power requirement is directly dependent upon the weight of the vehicle, and the weight of the vehicle is dependent upon the battery pack used in the series HEV. This means the power requirement of the HPAPU is coupled to the type of battery used. Starved electrolyte lead-acid batteries are commercially available with a specific energy of 35 W*hr/kg. Researchers [8, 9, 10] have shown that a specific energy of 55 W*hr/kg is possible with selected paste additives. The affect on vehicle performance and required HPAPU power by increasing the specific energy of the batteries is investigated next.

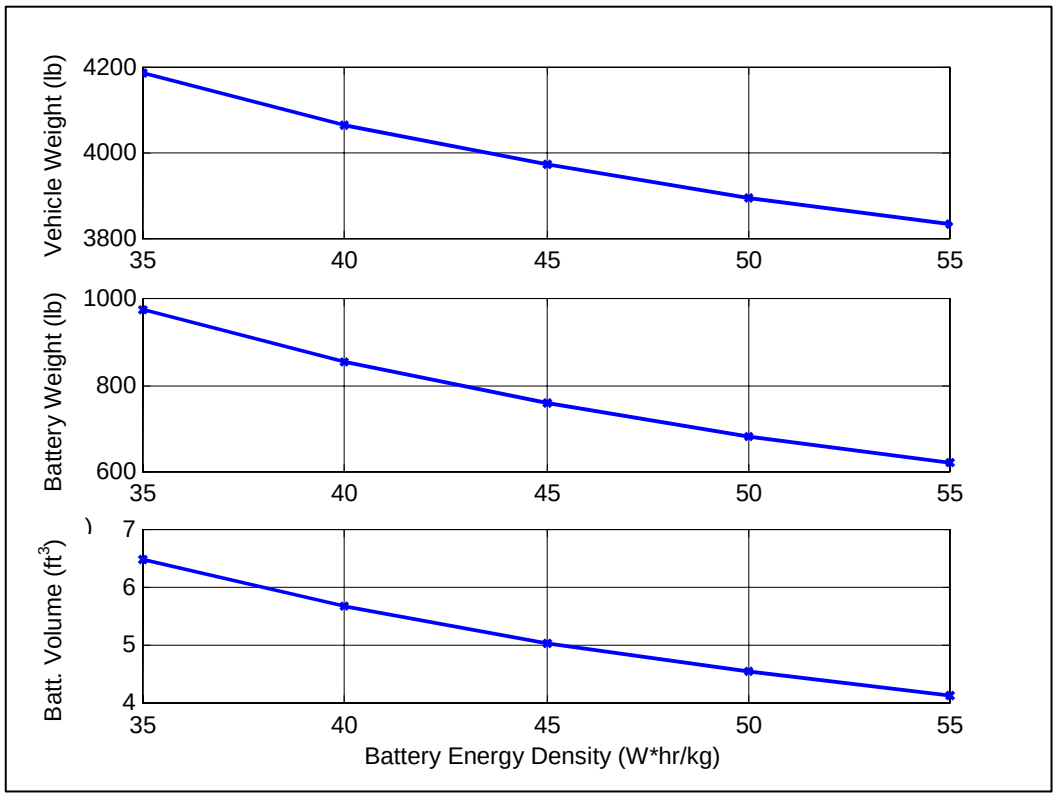

Figure 1.1 Vehicle properties versus battery pack energy density

1.1.5 Parametric Study of Specific Energy

A program called *roadload.m* was used to conduct a parametric study of the battery pack specific energy and its affect on the size and weight of the battery pack. In all cases, the battery

pack was required to meet the 60 mile zero tailpipe emission range. The specific battery pack energy density was varied from 35 to 55 W*hr/kg in 5 W*hr/kg increments.

Figure 1.1 shows that the weight of the battery pack ranged from 975 to 620 pounds as the specific energy increases. The volume of the battery pack is reduced by about 2.5 cubic feet as the specific energy density increases from 35 to 55 W*hr/kg. The overall vehicle weight is 4235 pounds with a 35 W*hr/kg battery pack and 3880 pounds with a 55 W*hr/kg battery pack. The affects of a battery pack with increased specific energy on the required APU power and fuel economy are investigated later in this chapter.

1.2 High Performance APU Design

The function of the HPAPU is to provide the power required by a series HEV for continuous highway driving. The power output of the HPAPU is determined by the steady state power requirement of the vehicle. This section outlines how the power requirement of the HPAPU was determined, specifies the components of the HPAPU and estimates the steady state fuel economy of the series HEV design while it is powered by the HPAPU.

1.2.1 Road Load Power Requirement

The power required from the HPAPU is dependent upon the weight, shape, and rolling resistance of the series HEV it is powering. The weight of the vehicle is dependent on the weight of the battery pack. The weight of the battery pack is dependent upon the speed and range requirements of the vehicle and the energy capacity of the battery pack. This makes the steady state power requirements of a series HEV a function of the speed and range requirements. A steady state road load model was developed using Matlab to handle this situation.

In the previous section, Eq. 1.1 was used to determine the required mass of the battery pack for a given set of specifications for range, road load power, battery pack specific energy, and the steady state vehicle velocity. The program *roadload.m* adds the weight of the battery pack, which was determined by Eq. 1.1, to the shell weight of the vehicle to find the total weight of

the vehicle. The total weight of the vehicle is used in the road load equation (Eq. 1.2) to determine the required power of the HPAPU as a function of velocity. The program can graphically display the required power versus velocity, as shown in Fig. 1.2.

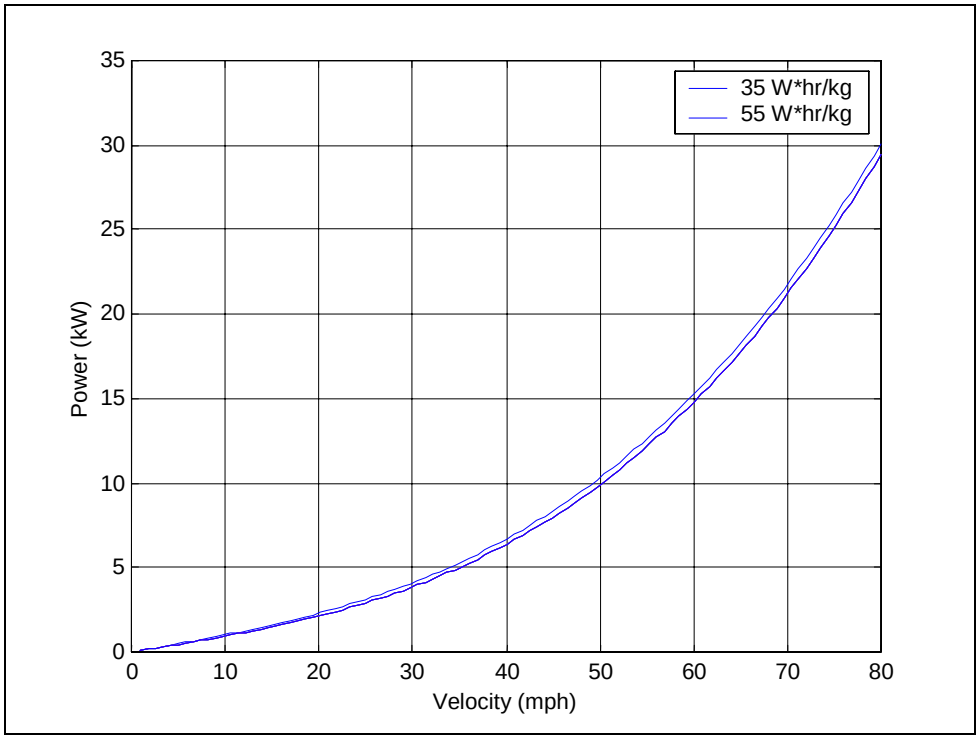

Figure 1.2 Road load power requirement

Figure 1.2 displays the road load power requirement for the two battery pack configurations. Both of these configurations use a vehicle shell weight of 3260 pounds (Table 1.3) and meet the requirement of 60 miles at 55 mph. The difference in these two configurations is the specific energy of the batteries. The solid line is for a battery pack with a specific energy of 35 W*hr/kg, and the dashed line is for a battery pack with a specific energy of 55 W*hr/kg. The weight difference between these two vehicle configurations is 355 pounds, the 35 W*hr/kg being the heavier of the two. With the 35 W*hr/kg battery pack the required power at 55 mph is about 12.5 kW. By using the 55 W*hr/kg battery pack the required power is reduced by 0.5 kW. The difference in required power is only 3 percent and does not affect the design of the HPAPU.

1.2.2 APU Design Philosophy

Two components that are required for a HPAPU are a four-stroke spark ignition (SI) engine and an alternator. High specific power and power density are desired from these two components so that the power requirements of the series HEV are met while minimizing the size and weight of the HPAPU. The HPAPU design principal achieves high specific power and power density by operating the SI engine and alternator at a high speed.

It has been experimentally proven that smaller displacement engines have a higher power to weight ratio [11]. Assuming that similar engines have the same indicator diagram (pressure vs. crank angle), the weight of an engine for a given displacement is proportional to the bore cubed, and the power output is proportional to the bore squared [11]. This means that the power output per pound, or specific power, has the trend of increased specific power with decreasing engine bore size. Smaller displacement IC engines tend to have smaller bores than larger displacement IC engines. Using a small displacement engine in this model serves the goal of an overall APU system with increased power output and reduced volume.

Small SI engines are not as efficient and clean as larger engines that have been engineered and optimized to meet the stringent emission and performance requirements of passenger vehicles. It seems possible to make improvements in the emissions and fuel efficiency of small 250-600 cc engines. This projection is based on Honda's success at achieving the Ultra Low Emissions Standards (ULEV) set by the California Air Resource Board with their line of Civic automobiles [12]. The Honda Civic uses a relatively small 1668 cc engine. Achieving ULEV standards with even smaller four-stroke engines presents an area for further research. The reason for the low amount of research in this area is the limited emission requirements on applications that use small four-stroke engines.

To achieve the desired power output from small engines, they must run at or above 6000 RPM. This presents some issues that require more research, such as the lifespan of the engine. Operating in excess of 6000 rpm will result in many more cycles of operation than in a slower revving conventional automobile or APU application. The internal bearing forces will be close

to the same as a large engine operating at slower speeds because the engine parts are smaller and weigh less [11]. The duty cycle of the engine will be relatively short since the series HEV will operate primarily as a ZEV. If the series HEV used grid electricity for 80 percent of its operation, the HPAPU would only be run for 20 percent of the vehicle's lifespan.

In addition to life, another major concern with using small, high-speed engines for this application is that of noise pollution. An engine operating at high speeds tends to create a large amount of noise. High-speed engines are typically used in applications where space is at a premium, such as on a motorcycle. They also tend to operate over a wide speed range. Both of these factors make it difficult to design muffling systems that will result in noise emissions similar to automobiles. This APU design and control strategy will operate the SI engine at approximately the same speed. This opens up the opportunity to design intake and exhaust systems that will greatly dampen the frequency of noise created at the operating speed by using Helmholtz resonators [13, 14, 15]. This should reduce the amount of noise emission to a reasonable level.

At a speed of 55 mph, the required steady state power is about 12.5 kW, or 16 hp for a series HEV using both the 35 and 55 w*hr/kg battery packs. This is graphically displayed in Fig. 1.2. Both engines shown in Table 1.4 [16] provide enough power to sustain a constant 55-mph. The 250cc engine is capable of a maximum power output of 30 kW, which is sufficient for a steady state operating speed of 80 mph. These Yamaha engines were chosen for consideration because they have the highest power density and specific power of all commercially available engines in the 200 - 450cc displacement range. Although these engines provide good performance, further volume and weight reductions would be possible with engines that were developed specifically for application in HPAPU systems.

Table 1.4 Yamaha Engine Specifications

Yamaha 4-Stroke Engine Specifications				
Engine	**Disp. (cc)**	**Type**	**Max. Power (kW)**	**RPM @ Max. Power**
YZ426FN	426	4-stroke, SI	42.7	9000
YZ250FN	250	4-stroke, SI	30.5	8500

Alternators tend to increase power output as their rotational speed increases. They also tend to increase power output as their volume and mass increases. For a given power output, an alternator could be larger and spin slowly or could be smaller and spin faster. This relationship will be exploited to increase the power density of the HPAPU by using a small, high-speed alternator design. The SI engine will be directly coupled to the alternator and the output of the rectifier will be connected to the high voltage bus.

1.2.3 HPAPU Component Selection

Two engines that will deliver the required 20-30 kW of power are shown in Table 1.4. Both of these engines are four-stroke spark ignition engines used in Yamaha Motor Corporation off-road motorcycles [16]. The 250cc engine was chosen for this design because it will supply enough power for maintaining the series HEV at a steady state velocity of 80 mph, which is an acceptable maximum cruising speed on any freeway in the U.S., and it is smaller and lighter than the 426cc engine.

The 250cc Yamaha engine has a rough external measurement of .35 x .41 x .51 meters, not including the exhaust system. This makes the overall volume of the engine approximately .073 cubic meters (2.6 cubic feet). An approximate dry weight for this engine, including a 5-speed transmission and cooling pump is 27 kg (60 pounds). Using this engine in a HPAPU system would not require a transmission, further reducing the weight of this engine for this application.

Fisher Electric Technology, Inc., has completed a design of a three phase, permanent magnet, 450 VAC alternator that is rated for 30 kW output at 7000 RPM [17]. The dimensions of the alternator are approximately 8 inches in diameter and 8.25 inches in length, with an approximate weight of 12.5 kg (30 pounds), including a full bridge rectifier. The volume of this alternator is approximately .007 cubic meters (.24 cubic feet).

1.2.4 Steady State Fuel Efficiency

Another function of the *roadload.m* program is to calculate the steady state fuel economy compared to vehicle velocity from the average specific fuel consumption (SFC) of the APU.

The fuel mileage for a series HEV was calculated by assuming that the energy produced by the APU is used directly by the electric propulsion system and that the APU control system produces just enough power for steady state operation at any given vehicle velocity. By using the road load equation, the required power is found for any given steady state velocity. The required power is then used in Eq. 1.3 to determine the fuel efficiency of the vehicle in miles per gallon. Equation 1.3 requires average specific fuel consumption in grams per kilowatt-hour and the average velocity of the vehicle in miles per hour. By making the equation for road load power a function of velocity and inserting it into Eq. 1.3, the fuel efficiency of an automobile is found as a function of vehicle velocity.

$$mpg = \frac{velocity \times 2827.8 \frac{grams}{gallon}}{SFC \times req.\ power} \tag{1.3}$$

To estimate the steady state fuel economy of the two series HEV battery pack configurations, the program *roadload.m* was used. They are both powered by the same HPAPU and the same specific fuel consumptions are assumed for both configurations. The specific fuel consumption (SFC) is assumed to be in the range of 300 to 330 g/kW*hr, which represents a best estimate for the engine fuel economy. With the present level of performance of small displacement IC engines, but with the addition of fuel injection and operating as a lean-burn engine, a SFC of 330 g/kW*hr seems attainable. This is based on information in Blair [13, 14] and Heywood [5], where normally aspirated, small displacement engines are shown to have specific fuel consumptions of around 400 g/kW*hr. Also, under ideal conditions, the dynamic engine model predicted a SFC of 178 g/kW*hr for the 250cc Yamaha engine.

The dynamic engine model that is presented in Section 3 has the capability to calculate the average SFC of an engine. It predicted that the 250cc Yamaha engine under throttled conditions with an average power output of 15 kW would have a SFC of 178 g/kW*hr. This predicted SFC is much lower than any SI engine is capable of attaining. The reasons why the engine model predicts such a low SFC is because heat transfer through the cylinder walls, engine friction, and pumping work are neglected, and the fuel injection system is assumed to be ideal.

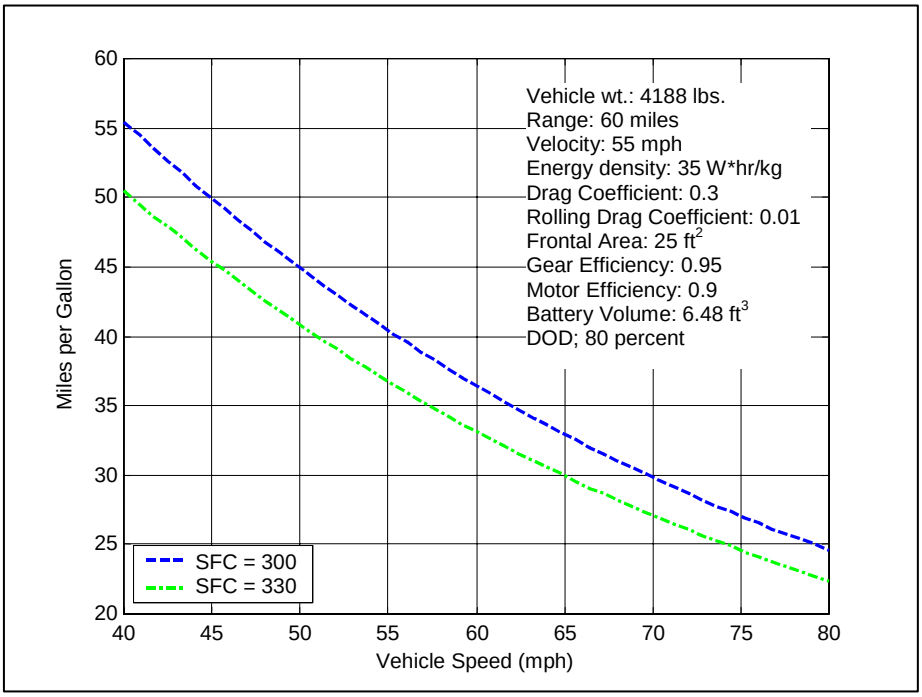

Figure 1.3 Highway fuel economy, 35 W*hr/kg

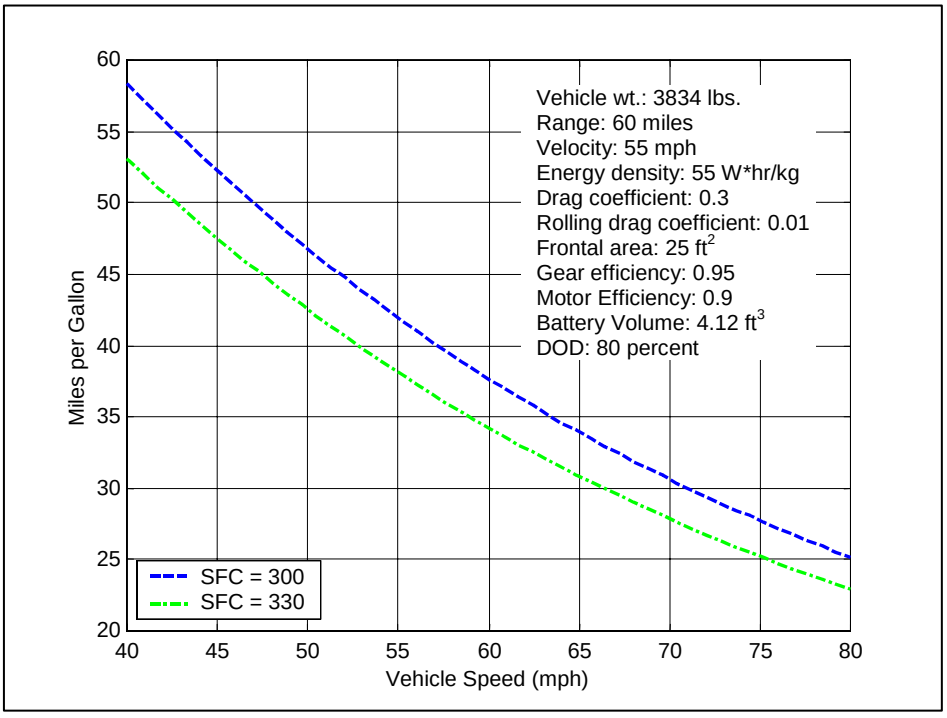

Figure 1.4 Highway fuel economy, 55 W*hr/kg

Figure 1.3 and Fig.1.4 graphically show the fuel economy information for series HEV with a 35 W*hr/kg and 55 W*hr/kg battery. At 55 mph the series HEV design using 55 w*hr/kg batteries is estimated to have a fuel economy in the range of 38 to 42 miles per gallon. The additional 355 pounds of batteries required by the 35 W*hr/kg versus the 55 W*hr/kg battery only changes the estimated fuel economy at 55 mph by two miles per gallon. This is approximately a 5 percent reduction in fuel economy.

1.3 Summary

In this section, a series HEV with a HPAPU was designed to provide the same or better range, fuel economy and acceleration performance as a 2001 Ford Taurus. The series HEV was 848 pounds heavier than the stock Taurus, but had a 60 mile zero tailpipe emission range, allowing approximately 80 percent of daily driving situations to be performed as an electric vehicle using grid electricity. The use of grid electricity reduces the emissions of the series HEV and moves the point of pollution formation away from population centers and to the point of energy production.

The series HEV uses a small, high-speed engine and alternator combination called a high performance auxiliary power unit (HPAPU) for extended range operation. Even though the engine is smaller and less fuel-efficient than the engine in the Taurus, the fuel economy is predicted to be slightly higher than the stock Taurus. This is because the engine can operate under more efficient conditions because it is decoupled from the traction wheels.
The effects of higher specific energy battery packs on vehicle performance and required HPAPU power were investigated. The weight difference between using a battery pack with a 35 W*hr/kg battery pack and a 55 W*hr/kg battery pack is 161 kg (355 pounds), the 35 W*hr/kg battery pack being the heavier of the two. The additional 355 pounds of batteries required by the 35 W*hr/kg battery pack increases the road load at 55 mph by 0.5 kW and decreases the estimated fuel economy at 55 mph by two miles per gallon when compared to the 55 W*hr/kg battery pack. The weight that would be saved by using a battery pack with a higher specific energy did not affect the design of the HPAPU because of the small (3 percent) reduction in the steady state power requirement.

Using a Yamaha YZ250FN 4-stroke, SI engine coupled to the 30kW Fisher alternator specified above, the HPAPU will weigh 41 kg (90 lbs.) and occupy a volume less than .09 cubic meters (3 cubic feet), not including the cooling or exhaust systems. The HPAPU will output a maximum of 30 kW of electric power at an operating speed of 8500 RPM, which is enough power to maintain the series HEV presented in this chapter at a speed of 80 mph. An electric power output from the HPAPU of 17 kW will maintain the series HEV at a steady 65 mph.

2.0 Dynamic Engine Model

The engine simulation program is based on a one-dimensional heat release closed cycle engine model and a compressible fluid throttle body model. The code was written for Matlab version 5.3. The program structure is broken up into a main simulation control and parameter entry m-file, and three function m-files. The simulation control code *run_sim.m* controls the size and number of time steps and provides a single entry point for all engine specific variables and operating condition variables. All variables used by the functions are global variables and therefore only need to be changed in *run_sim.m*. The output of the engine simulation program is average torque, average power, rotational speed and intake manifold pressure in the time domain.

The three functions are named *control.m*, *intake.m* and *engine.m*. *Run_sim.m* calls each of these functions to perform calculations needed for the next time step in the simulation. *Control.m* is a proportional/derivative (PD) controller used for closed loop speed control. *Intake.m* performs throttle body and intake manifold calculations. *Engine.m* is the closed system combustion routine, and the rotational dynamics are handled in the main control program, *run_sim.m*.

Figure 2.1 is a control loop diagram for the *run_sim.m* code. It shows the major variables passed from function to function and the overall program flow. The rotational dynamics and the τ_{load} input are both handled within *run_sim.m*. In a complete APU simulation, τ_{load} would be generated by the alternator model and passed to the engine model.

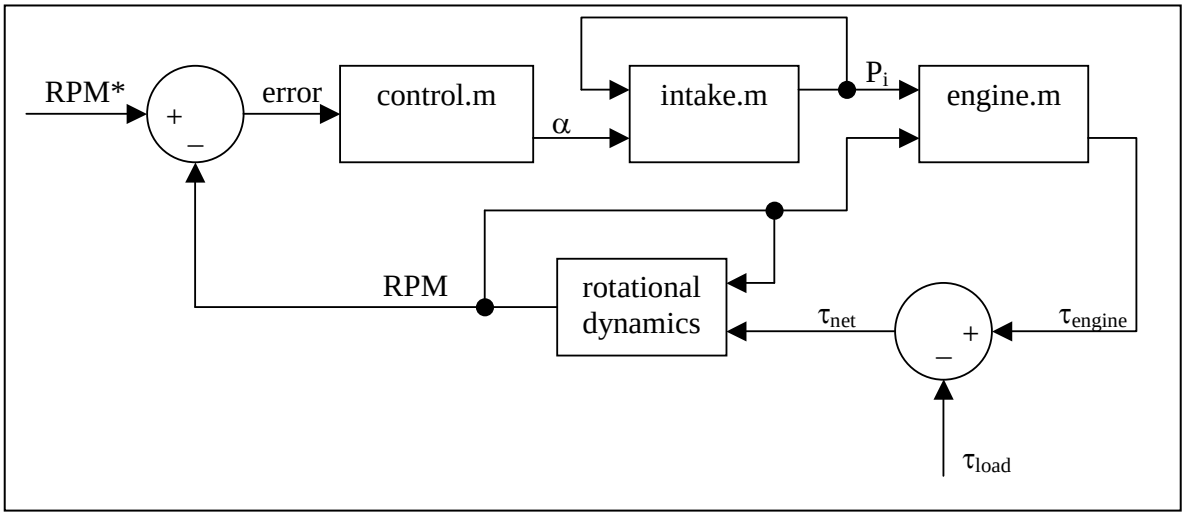

Figure 2.1 Engine simulation control loop and code structure

Parts of this simulation are backwards looking predictive models. This means that calculations are made based on the conditions of the last time step to make a prediction for the present time step. *Intake.m* and the rotational dynamics both do this. This introduces some error into the transient analysis, but it is not significant compared to other aspects of the model. The primary purpose of this engine model is to behave in a similar manner to a real IC engine with the same dimensions entered into the model, but not to make accurate predictions of dynamic intake manifold pressure.

Features of this model include dimensioned engine specification input, time steps for each combustion event and closed loop control capability. This model provides output in the time domain and is intended to be one part of a complete HPAPU dynamic simulation tool. The engine model would need to interact with a model for the alternator and battery.

The engine model can be used to analyze both two and four-stroke spark ignition (SI) engines having multiple cylinders and any engine displacement. For this project, a 250cc displacement, one cylinder, four-stroke, (SI) engine was analyzed. Table 2.1 lists the engine specific inputs for the model as they are listed in the Matlab code. Figure 2.2 helps identify the physical dimensions bore, stroke, Lcr and Lp.

The engine model was developed for the purpose of giving reasonable estimates for the performance of an internal combustion engine. This model is simple, runs quickly, and accepts dimensioned engine specifications. Details that this model includes are non-ideal airflow past the throttle body, and volumetric efficiency losses through the intake manifold and valves, and could be extended to include fuel injection control and emission estimates.

Table 2.1 Engine Specific Model Inputs

Variable Name	Description
bore	diameter of pistons
stroke	stroke of pistons
CR	compression ratio
n	number of cylinders
nr	number of cycles per power stroke (4-stroke = 2; 2-stroke = 1
Lcr	connecting rod length
Lp	distance from gudgeon pin to piston face
eta_V	volumetric efficiency of engine
J	Effective moment of inertia of the engine and load

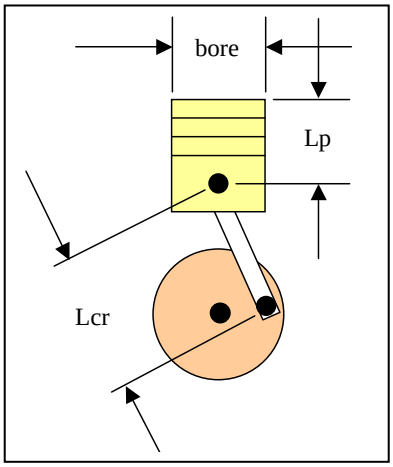

Figure 2.2 Physical engine dimensions

2.1 Throttle Body

The most common throttle body used on spark ignition engines is the butterfly valve. Figure 2.3 shows an end view and a cross section view of a butterfly valve assembly. Its purpose is to limit the flow of air into the intake manifold and ultimately the combustion chamber. By limiting the airflow into the engine, the power output of the engine is controlled, or throttled. The amount of throttling by the butterfly valve is modeled assuming real compressible flow in the model. It is the only control implemented in this engine model.

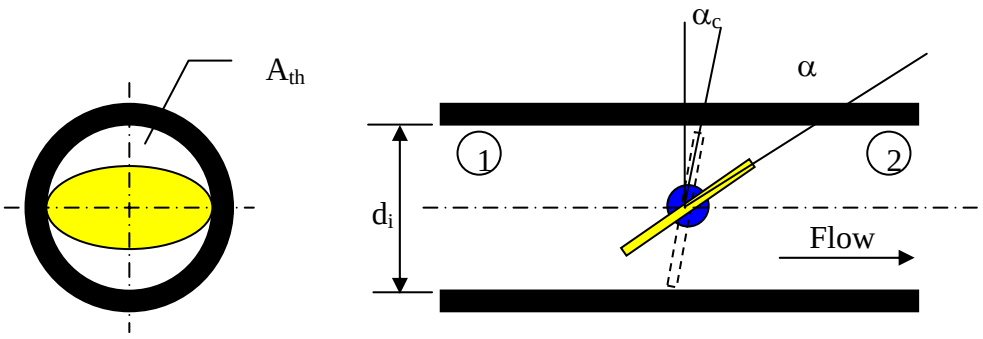

Figure 2.3 Butterfly valve throttle body

Since the flow of air past the throttling device is compressible, the mass flow through the butterfly valve depends on the pressure difference across the throttling plate, up to a certain point. Beyond this point, no higher mass flow rate can be achieved past the throttle plate. This point is called the critical pressure ratio [5] and is related to the point at which the airflow speed past the throttle plate reaches the speed of sound. Upon reaching the speed of sound, the pressure waves created by the supersonic flow effectively reduces the open throttle area A_{th}.

This behavior of the compressible flow divides the function for mass flow through a butterfly throttle body into a non-linear, piecewise continuous system. When operating above the critical pressure level, the equations for real compressible fluid flow must be used. When operating at or below the critical pressure level, the equations for choked flow must be used. Both the choked flow and non-choked flow regimes are modeled in this engine model.

2.1.1 Critical Pressure Ratio

The critical pressure ratio p_{cr} is defined as the ratio of the down stream pressure over the upstream pressure, or in Fig. 2.3 the pressure at point 2 divided by the pressure at point 1. The exact value of the critical pressure depends on the specific heat ratio of the fluid. This engine model assumes distributed fuel injection at each intake valve, so only air passes through the throttle body and the assumption of an ideal gas, air, is appropriate for the fluid passing through the throttle body; the specific heat ratio of air γ is1.4 and results in a critical pressure ratio of 0.528 [5].

2.1.2 Non-Choked Flow

For pressure ratios above the critical pressure ratio, the equation used to find the mass flow of air past the throttle plate is that for real compressed fluid flow (Fig. 2.1) [5]. In Eq. 2.1 $\dot{m}_{th}$ is the mass flow rate of air past the throttle plate, A_{th} is the open area of the throttle body, C_D is a discharge coefficient or efficiency, p_o and T_o are the ambient pressure and temperature, R is the universal gas constant, γ is the ratio of specific heats, and p_{im} is the pressure on the down stream side of the throttle plate in the intake manifold. The discharge coefficient is a term that must be experimentally found for each geometric shape and can change in value depending on the mass flow rate and the down stream pressure.

$$\dot{m}_{th} = \frac{C_D\, A_{th}\, p_o}{\sqrt{RT_o}} \left(\frac{p_{im}}{p_o}\right)^{1/\gamma} \left\{\frac{2\gamma}{\gamma-1}\left[1-\left(\frac{p_{im}}{p_o}\right)^{(\gamma-1)/\gamma}\right]\right\}^{1/2} \tag{2.1}$$

2.1.3 Choked Flow

For pressure ratios across the throttle less than the critical value, the mass flow past the throttle plate depends only upon the discharge coefficient and the open throttle area. Since this model assumes a constant discharge coefficient, the mass flow depends only on the open throttle area. Equation. 2.2 is the equation for choked flow past a butterfly valve [5].

$$\dot{m}_{th} = \frac{C_D\, A_{th}\, p_o}{\sqrt{RT_o}}\, \gamma^{1/2} \left(\frac{2}{\gamma+1}\right)^{(\gamma+1)/2(\gamma-1)} \tag{2.2}$$

2.1.4 Open Throttle Area

Most butterfly valves are manufactured with an elliptical throttle plate. As the throttle plate is rotated, its shape remains that of an ellipsis if viewed along the axis of the throttle passage. The equation for a butterfly valve with an elliptical throttle plate from Blair [13] is shown in Eq. 2.3 and is assumed to be close enough for the purposes of this model. α_c is the angle at which the throttle plate is fully closed and α is the angle of the throttle plate. The throttle angle is the control input to the engine model.

$$A_{th} = \frac{\pi d_i^2}{4}\left[1 - \frac{\cos(\alpha - \alpha_c)}{\cos(\alpha_c)}\right] \tag{2.3}$$

2.2 Intake Manifold

The intake manifold can be viewed as a section of air duct between the throttle body and the combustion cylinders. The throttle body controls airflow into the intake manifold. Intake valves, engine speed and specific engine parameters control the outflow from the intake manifold. These specific engine parameters are V_{im}, NR, N and η_V. V_{im} is the volume of the intake manifold and η_V is the volumetric efficiency of the intake manifold, valves and combustion chamber.

2.2.1 Volumetric Efficiency

To account for the non-ideal fluid flow inside of the intake manifold and cylinders, a term called volumetric efficiency is used. Volumetric efficiency η_V (eta_V in the Matlab code) is defined as the mass of air in the combustion chamber at the closing of the intake valve(s) divided by the mass of air that could be in the combustion chamber at the intake manifold pressure p_{im}. The volumetric efficiency term is used in Eq. 2.6 to account for the pressure drop from the intake manifold to the combustion chamber.

The pressure drop is caused by the effects of real compressible flow through the intake manifold, intake valves, three-dimensional flow in the combustion chamber during the intake stroke and the limited time for air to fill the cylinder. An accurate description of the fluid flow

inside of the intake manifold and cylinders would require a detailed description of the intake valve and combustion chamber geometry and would increase the model's complexity and computation time. In an initial attempt at modeling the flow through the intake manifold, a volumetric efficiency of 1.00 was used. This value resulted in good agreement to factory supplied power specifications.

2.2.2 Emptying and Filling Technique

The emptying and filling technique (the plenum method) is a method of analyzing the flow through the intake manifold using a control volume approach. Equation 2.7 was taken from Heywood [5]. This equation is a first order ordinary differential equation for the mass of air in the intake manifold m_{im}. The mass flow through the throttle body $\dot{m}_{th}$ is explained in the throttle body section of this chapter. The mass flow rate out of the intake manifold is the same as the sum of the mass flow rate into the cylinders.

$$\frac{dm_{im}}{dt} = \dot{m}_{th} - \sum \dot{m}_{cyl} \tag{2.4}$$

The emptying and filling technique can be thought of as a control volume analysis of the intake manifold volume V_{im} using the mass conservation part of the first law of thermodynamics. Integrating Eq. 2.4 with respect to time results in the mass of air in the intake manifold. By dividing the mass of air in the intake manifold by the volume of the intake manifold, which is constant, the density of the air inside of the intake manifold ρ_{im} can be found. Then the ideal gas law (Eq. 2.5) is used to find the intake manifold air pressure. R_{air} is the ideal gas constant for air and T_{im} is the temperature inside of the intake manifold.

$$p_{im} = \frac{R_{air}\, T_{im}}{\rho_{ai}} \tag{2.5}$$

2.2.3 Mass Flow Rate into Cylinders

The mass flow rate into the cylinders is found with Eq. 2.6. This equation has been adapted from Heywood [5] for use in this model. It takes into account the engine specific parameters

for two or four stroke operation, swept volume (based on the bore and stroke) and volumetric efficiency. In the Matlab code, the summation of $\dot{m}_{cyl}$ is handled by multiplying the right side of Eq. 2.6 by N, the number of cylinders in the engine.

$$\sum \dot{m}_{cyl} = \frac{\eta_V \ \rho_{im} V_{sv} \ RPM}{nr \cdot 60} \tag{2.6}$$

2.3 Steady State Performance Map

This chapter helps to illustrate the throttle body, intake manifold and mass flow equations and show how they relate to engine performance. Figure 2.4 is a steady state performance map for a 250 cc, four-stroke, spark ignition Yamaha motorcycle engine. It was developed with the Matlab code *mdot_press.m* and is not actual test data. This is important information for this model because all of the transients of engine operation are directly related to the density of the air inside of the intake manifold, except the rotational inertia of the engine and load.

This performance map shows the mass flow rate of air through the engine on the y-axis, pressure ratio on the x-axis, and lines of constant throttle angle and engine speed. The lines of constant throttle angle are the solid lines, and the dashed lines are of constant engine speed. The dashed vertical line shows the critical pressure for air at 0.528 on the x-axis.
Figure 2.3 shows that engine speed is not just a function of throttle angle. Engine speed is a function of throttle angle and the torque applied to the engine. A higher applied torque equates to a higher pressure ratio, up to a pressure ratio of nearly one. Pressure ratios above one signify a supercharged or turbocharged induction system, which this model is not designed to simulate. Notice in Fig. 2.4 that for a given throttle angle, the mass flow rate increases with decreasing pressure ratio up to the critical pressure ratio. The choked flow domain is to the left of the critical pressure ratio line in Fig. 2.4 and the non-choked flow is to the right. Though this is a steady state map of the engine performance, it demonstrates the critical pressure ratio and shows how all of the equations interact to describe the mechanics of the airflow into the combustion chamber during throttle conditions.

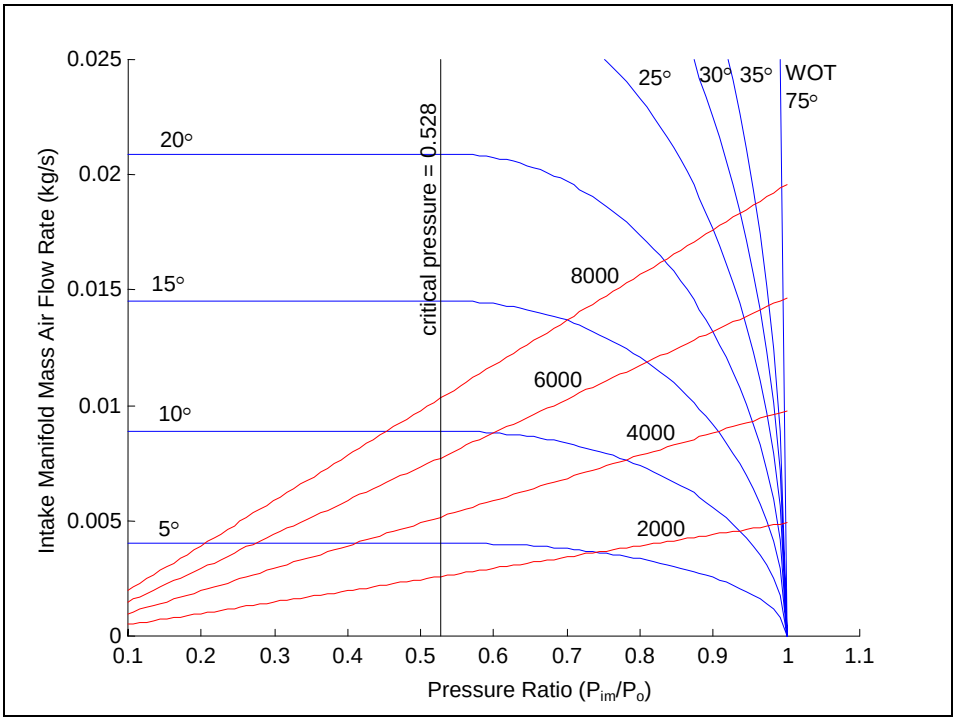

Figure 2.4 – Steady State Engine Performance Map

2.4 Closed System Combustion

During the combustion cycle of engine operation, the combustion chamber is closed to all mass transfer. The fuel/air mixture inside of the cylinder walls and piston head are trapped when the intake valve closes, sometime after bottom dead center (BDC). This mixture is compressed as the piston moves upwards, inputting work to the closed system. This increases the pressure inside of the combustion chamber. Ignition of the fuel/air mixture occurs just before top dead center (TDC). The combustion of the fuel/air mixture releases heat energy into the closed system. As the piston passes TDC, the pressure inside of the combustion chamber does work on the piston face, which is mechanically transferred to torque on the crankshaft of the engine. The simulation of this process uses a closed system thermodynamic model.

For the purposes of this model, the desired output of the engine model is average power, speed, and torque, not instantaneous power, speed and torque. Since only an average power is desired from the model, the actual pressure and temperature are not needed as output. However, because combustion in this piston cylinder system does not occur at constant pressure or

volume the first law of thermodynamics cannot be solved in one step. To accommodate this combustion process, the model makes discrete steps through the closed cycle combustion event recording pressure and combustion chamber volume (V) at each step. Each of these pressure/volume pairs is used to find the total work done on the piston by the compressing and expanding fuel/air mixture.

Equation 2.7 [18] is the equation for expansion and compression work. Using the definition of an integral, Eq. 2.7 can be approximated by Eq. 2.8. Equation 2.8 shows that the work of the closed combustion cycle is approximated by the sum of instantaneous pressures multiplied by the unit change of volume in the combustion cylinder ΔV. The smaller the ΔV used, the more accurate the integral approximation but at the cost of longer calculation time.

$$W = \int p \, dV \tag{2.7}$$

$$W = \sum_{i=1}^{n} p(V)_i \times \Delta V_i \tag{2.8}$$

The average power output is found by taking the amount of work output from a single combustion event and dividing it by the time it takes for a complete cycle of engine operation. A complete cycle of operation would be one revolution for a two-stroke engine and two revolutions for a four-stroke engine, and the time per revolution depends on the operating speed of the engine.

2.4.1 Combustion Chamber Thermodynamics

A closed cycle piston cylinder thermodynamic model is used to find the pressure as a function of crank angle θ. Pressure as a function of θ is desired because it is easier to work with because the valve and spark timing is always stated in terms of crank angle. Since the volume is only a function of crank angle, it is easy to shift mathematically from volume to crank angle.

The closed cycle is evaluated from the time the intake valve closes (θ_{ic}) until the exhaust valve opens (θ_{eo}). The engine crank angle is defined as zero at top dead center. The combustion

chamber is closed at some point after bottom dead center and the piston continues to move upward, reducing the volume of the combustion chamber and increasing the pressure and temperature of the trapped mixture. This continues until TDC, after which the piston moving downwards, increasing the volume of the combustion chamber, reduces the pressure. Just before TDC, a spark ignites the fuel/air mixture. This releases heat energy from the fuel. The heated gas inside the cylinder further increases the cylinder pressure as the piston moves downward. Heat energy of the trapped gas is does work on the piston, which converts the heat energy into mechanical energy in the form of torque on the crankshaft of the engine.

The first law of thermodynamics is used to describe the closed cycle combustion process (Eq. 2.9, where C_v is the specific heat content at constant volume m is mass of cylinder contents). It is in the form of: internal energy equals heat addition minus work and is expressed as an ordinary differential equation with respect to crank angle. The sign convention for work is positive work is out of the system, or in this case, positive work flows from the cylinder to the crankshaft:

$$m \cdot C_V \cdot \frac{dT}{d\theta} = \frac{dQ}{d\theta} - p \cdot \frac{dV}{d\theta} \tag{2.9}$$

For the use in this model, Eq. 2.9 must be rearranged into a differential equation for pressure with respect to crank angle. The steps to accomplish this are to find relationships for the differential terms $\frac{dT}{d\theta}$, $\frac{dQ}{d\theta}$ and $\frac{dV}{d\theta}$ in terms of known constants and variables, and then algebraically manipulate the equation to the desired format. The next subsections explain the details of finding the relationships of the differential terms.

2.4.2 Cylinder Volume

The volume of the combustion chamber is only a function of the crank angle θ and is shown in Eq. 2.10. This equation has been adapted from an equation of motion for a piston cylinder assembly from [18]. The clearance or squish volume V_{cv} is defined as the volume of the combustion chamber at top dead center and is determined by the compression ratio of the

engine CR (Eq. 2.11) and the engine displacement V_{sv}. The derivative of Eq. 2.10 with respect to crank angle is shown in Eq. 2.12. Equation 2.10, 2.11, and 2.12 are used in the model.

$$V(\theta) = \left[L_{cr} + L_{ct}(1-\cos\theta) - \sqrt{{L_{cr}}^2 - (L_{ct}\sin\theta)^2} \right] \left(\frac{\pi \times bore^2}{4} \right) + V_{cv} \quad (2.10)$$

$$V_{cv} = \frac{V_{sv}}{CR} \quad (2.11)$$

$$\frac{dV}{d\theta} = \left(\frac{\pi \cdot bore^2}{4} \right) \left[\frac{L_{ct} * \sin(\theta) + {L_{ct}}^2 \sin(\theta)\cos(\theta)}{\sqrt{{L_{cr}}^2 - {L_{ct}}^2 \sin^2(\theta)}} \right] \quad (2.12)$$

2.4.3 Heat Addition

Heat addition to the system comes from combusting the fuel/air mixture inside of the cylinder. The amount of heat generation is determined by the amount of fuel and air in the cylinder, the rate at which it burns and the amount of heat transfer through the cylinder walls. Heat transfer through the cylinder walls is neglected because it small compared to the total amount of heat generated and does not affect the characteristics of this model's response to inputs. It is significant enough that it should be included before a validation of this model is attempted.

A distributed fuel injection system is assumed for the fuel delivery system in this model. At present, the fuel injection model is for an ideal injection control system. This ideal injection control system always provides a stoichiometric fuel/air mixture. The pressure of the air drawn from the intake manifold determines the amount of fuel added to the air in the combustion chamber, and the mass of fuel in the combustion chamber determines the amount of heat that can be released from combusting the air/fuel mixture. In this model the heat energy released during combustion is found using Eq. 2.13. Equation 2.13 is used in the model to determine enthalpy, or added heat of the fuel based on the lower heating value (LHV) of the fuel.

$$Q_h = LHV \times m_{fuel} \quad (2.13)$$

The mass, or amount of fuel in the cylinder at intake valve closure, is determined from the density of fuel in the combustion chamber (ρ_{fi}) and the volume of the combustion chamber

(V_{ic}) when the intake valve closes. The density of the fuel in the combustion chamber is a factor of the density of air in the intake manifold and the air/fuel mixture ratio.

$$m_{fuel} = \rho_{fi} V_{ic} \tag{2.14}$$

$$\rho_{fi} = \frac{\rho_{im}}{\left(\frac{A}{F}\right)} \tag{2.15}$$

Air/fuel ratios used in engines are based on the stoichiometric ratio of the fuel used. That is, the mass units of air per mass unit of fuel for perfect combustion, neither lean nor rich. The stoichiometric ratio $\left(\frac{A}{F}\right)_S$ of gasoline is about 13.7. This model uses the equivalence ratio, λ, to determine the actual air/fuel ratio in the combustion chamber (2.16). This will facilitate future improvements in the fuel injection model to include a non-ideal fuel injection control.

$$\left(\frac{A}{F}\right) = \left(\frac{A}{F}\right)_S \lambda \tag{2.16}$$

The air inside of the intake manifold is treated as an ideal gas. As such, the density can be found by manipulating the ideal gas law. The pressure of the air in the intake manifold is covered in the throttle body section.

The air/fuel mixture is combusted to release heat. As stated earlier, this process does not occur at constant pressure or constant volume because the piston is always moving. This creates a situation where the timing of the heat release is critical. A model that is commonly used to describe the rate of heat release in a combustion chamber is called the Weibe function.

2.4.4 Weibe Function

The Weibe function is used to define heat addition term $\frac{dQ}{d\theta}$ and is an exponential equation representing 0 to100 percent of the fuel being burnt as a function of crank angle. The heat addition term (Eq. 2.17) is simply the derivative of the Weibe function with respect to crank

angle multiplied by the enthalpy of the fuel in the combustion chamber, assuming the heat loss term is neglected.

$$\frac{dQ}{d\theta} = Q_h \frac{dx_B}{d\theta} \tag{2.17}$$

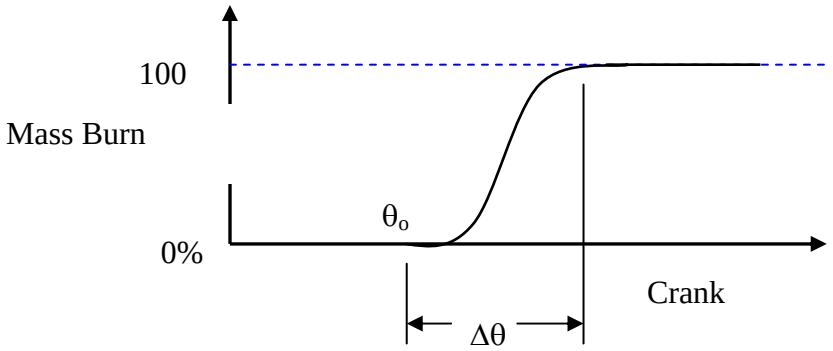

Figure 2.5 Weibe function

Inputs to the Weibe function include the crank angle of ignition (θ_o), the burn duration ($\Delta\theta$) and some coefficients (a, m). The coefficients a and m change the shape of the curve and can be experimentally fitted to a specific engine's combustion characteristics. Heywood [19] has shown that actual mass fraction burned curves have been fit to a = 5 and m = 2, but for present level of model performance, the value of the Weibe function coefficients are not critical.

$$x_B(\theta) = 1 - \exp\left[-a\left(\frac{\theta - \theta_o}{\Delta\theta} \right)^{m+1} \right] \tag{2.18}$$

2.4.5 Algebraic Manipulation

With some algebraic manipulation, Eq. 2.9 can be reworked to a differential equation for the combustion chamber pressure as a function of crank angle. The first manipulation requires the assumption that the air/fuel mixture inside the combustion chamber is an ideal gas. This assumption is only valid for an ideal engine model and neglects many details required for an accurate in cylinder pressure prediction. For this application, only an approximate pressure

profile is needed to find a total work output of a combustion event. Using the ideal gas law (Eq. 2.19 [18]) and the relationship of the specific heat of an ideal gas (Eq. 3.20 and Eq. 3.21 [18]), Eq. 2.9 can be reworked into the form of Eq. 2.22.

$$p \cdot V = m \cdot R \cdot T \tag{2.19}$$

$$c_p - c_v = R \tag{2.20}$$

$$\frac{c_p}{c_v} = \gamma \tag{2.21}$$

$$\frac{dT}{d\theta} = T(\gamma - 1)\left[\frac{1}{p \cdot V}\frac{dQ}{d\theta} - \frac{1}{V}\frac{dV}{d\theta}\right] \tag{2.22}$$

Equation 2.22 still requires some manipulation and a substitution. The $\frac{dQ}{d\theta}$ and $\frac{dV}{d\theta}$ terms have been explained in the previous subsections. To simplify the equations, they will not be substituted into the following equations. The $\frac{dT}{d\theta}$ term requires another manipulation, once again using the ideal gas law.

Replacing $\frac{dT}{d\theta}$ with $\frac{dp}{d\theta}$ is the next step. Starting with the ideal gas equation, Eq. 2.18 arrives at Eq. 2.23 by taking derivative with respect to crank angle of both sides of the equation. Equation 2.23 can be rewritten as Eq. 2.24 with some more ideal gas law and algebraic manipulation. Equation 2.22 is then substituted for the $\frac{dT}{d\theta}$ term. The result is a differential equation for the combustion chamber pressure as a function of crank angle during closed system combustion (Eq. 2.25). Equation 2.25 is used in the dynamic engine model.

$$V\frac{dp}{d\theta} + p\frac{dV}{d\theta} = m \cdot R\frac{dT}{d\theta} \tag{2.23}$$

$$\frac{dp}{d\theta} = -\frac{p}{V}\frac{dV}{d\theta} + \frac{p}{T}\frac{dT}{d\theta} \tag{2.24}$$

$$\frac{dp}{d\theta} = -\frac{\gamma\, p}{V}\frac{dV}{d\theta} + (\gamma - 1)\frac{Q_h}{V}\frac{dx_B}{d\theta} + (\gamma - 1)\frac{1}{dV}\frac{dQ_L}{d\theta} \tag{2.25}$$

2.5 Average Torque and Power Output

For each combustion event, the total amount of work output is calculated. The average power output is found by taking the amount of work output from a single combustion event and dividing it by the time it takes for a complete cycle of engine operation. The length of the time step depends on the amount of time it has taken for complete cycle of operation. A complete cycle of operation would be one revolution for a two-stroke engine and two revolutions for a four-stroke engine and is determined by the engine specific variable, nr.

2.5.1 Model Time Step

Calculating the model time step is a straightforward calculation. The time step is the inverse of engine speed with terms in the numerator to make the units correct and to account for two or four-stroke operation. The 60 in the numerator is used to give the time step units of seconds while using the engine speed in terms of rotations per minute (RPM).

$$dt = \frac{60 \times nr}{RPM} \tag{2.26}$$

2.5.2 Average Power Output

The total work output of the combustion stroke (Eq. 2.8) is divided by the time step (Eq. 2.26) to find the average power output for each complete engine cycle. This method does not include pumping work to remove the exhaust from the combustion chamber or drawing in a fresh air/fuel charge. It also neglects engine friction. Engine friction would be a relatively simple addition to the model since the empirical equations are only a factor of engine speed. Friction was neglected to simplify and speed up the model calculation.

$$\dot{W}_{ave} = \frac{\sum_{i=1}^{n} p_i \times \Delta V_i}{dt} \tag{2.27}$$

2.5.3 Average Torque Output

The average torque of a shaft is defined as the average power output of the shaft divided by its angular velocity. Average power output is found with Eq. 2.27, and the angular velocity of the shaft is directly related to the speed or RPM of the engine. In this model, the average torque output of the engine is defined by Eq. 2.28.

$$\tau_{ave} = \frac{\dot{W}_{ave} \cdot 30}{RPM \cdot \pi} \tag{2.28}$$

2.6 Rotational Dynamics

The power output of the IC engine can either be converted to electric energy by the alternator or it can accelerate the engine and alternator speed. The amount of power that goes towards accelerating the engine depends on the power output of the engine and the load on the engine from the alternator. If the load on the engine is less than the torque output of the engine, the engine will accelerate; if the load on the engine is more than the torque output of the engine, the engine will decelerate. Equation 2.29 and Eq. 2.30 are used to find the angular acceleration of the engine and alternator, where J is the rotational inertia of the engine and the alternator.

$$\tau_{net} = \tau_{engine} - \tau_{load} \tag{2.29}$$

$$\frac{d\omega}{dt} = \frac{\tau_{net}}{J} \tag{2.30}$$

This engine model incorporates real compressible fluid flow for throttled operation and a heat release combustion model to find the work output of each combustion event. Torque and power output from each combustion event is averaged over time to find the average toque and power output of the engine. The real compressible fluid flow model captures the power and torque transients present during throttled operating conditions. Power and toque transients result in fluctuations in the engine speed.

2.7 Dynamic Engine Model Results

The contents of Section 3 include the results of the engine model validations and closed loop speed control of the engine model. The engine model was validated in two different ways. First, the power output of the engine model was compared to a single operation point of a 250cc Yamaha motorcycle engine, and second, the behavior of engine model parameters were observed while a step change in the throttle angle was made. After the engine model showed reasonable behavior, closed loop speed control was implemented. Two test cases were performed on the engine model under closed loop speed control; these conditions were a step and ramp change in the torque applied to the engine model.

2.7.1 Single Point Engine Model Validation

For a single point validation of the model, the specifications for a Yamaha YZ250FN engine were entered into the engine model. The throttle was set to wide-open throttle (WOT), which is 75° for this engine, and the load on the engine was adjusted until a steady operating condition of ≈ 8500 RPM was reached. The results showed a constant power output of 30.8 kW at 8561 RPM, which is close to the specifications shown in Table 3.2 of 30.5 kW at8500. This result helps validate the accuracy of this engine model, though a higher power output was expected from the model since heat loss from the cylinder and friction terms have been neglected.

The most likely reason for the lower than expected power output from the model is that the discharge coefficient (C_D) of the throttle body was set too low for WOT conditions, since the volumetric efficiency was set as 1.00. In reality, the discharge coefficient varies depending on the mass flow rate and pressure drop across the throttle plate, for which this model does not account. A higher discharge coefficient would increase the intake manifold pressure and in turn the power output of the engine model. It does point out that this model can be adjusted to match a set of engine data if the volumetric efficiency term is adjusted. However, this would not be an acceptable solution if fuel consumption or emission components were added to this model.

Another reason for not having a higher power output from the model could be caused by not accounting for intake manifold dynamics. With the correct intake manifold design, the air/fuel mixture can be forced into the combustion chamber by harmonic resonance just before the intake valves close [5, 13, 14]. This effect increases the initial pressure of the combustion process and increases the maximum power output of the engine. The engine model does not account for intake manifold harmonics.

2.7.2 Engine Model Behavior Validation

To validate the behavior of the IC engine model, a series of perturbations were done on the load and the throttle angle of the engine under open loop operation. These perturbations simulate changes in the independent variables, throttle angle and load torque. The changes in the dependent model variables were compared to a real IC engine in order to validate the general model behavior. Additionally, the magnitude of the model responses is compared to real engine data. For this validation, the specifications for a Yamaha YZ250FN four-stroke motorcycle were used (see Table 3.1) [16].

Table 3.1 YZ250FN Engine Specifications

Displacement	249 cc
Bore	77 mm
Stroke	52.6 mm
CR	12.5:1
Power	30.5 kW @8500 RPM

The RPM response profile of Fig. 3.1 supports the validity of the model by gradually increasing from the point in time when the throttle angle is increased until the throttle angle is decreased. The change is expected to be gradual since the engine has rotating inertia and is under a constant load. Shortly after the point the throttle is stepped down, the RPM begins decreasing, which is expected of a real engine.

If a constant load is applied to the engine and the throttle is suddenly opened more, an increase in the intake manifold pressure would be expected. This is because there would be less

restriction by the throttle plate, resulting in a lower pressure drop across the throttling device. With a lower pressure drop a higher mass flow will be entering the intake manifold. Since the engine has rotating inertia, the engine speed will not immediately increase. The result is a positive mass flow rate into the intake manifold, resulting in an increase in the intake manifold pressure. Furthermore, it is expected that the intake manifold pressure will initially change very quickly to a step change in the throttle angle position, followed by a gradual reduction in the rate of change of the intake manifold pressure due to the engine speeding up and the mass flow rate through the intake manifold reaching equilibrium.

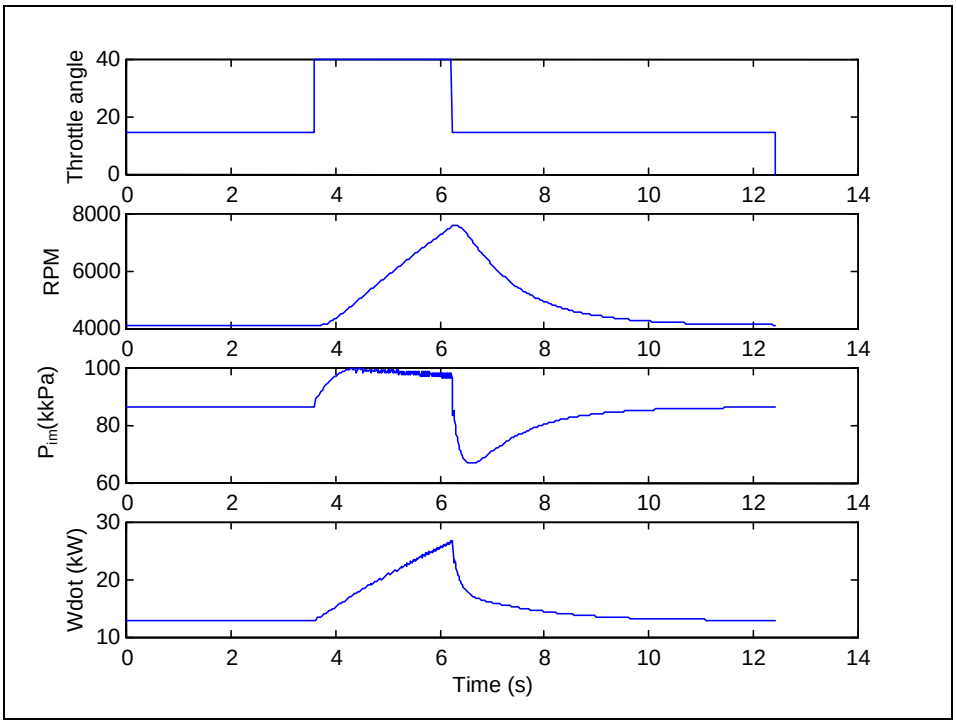

Figure 3.1 Open loop throttle control

Figure 3.1 shows the intake manifold pressure response to step changes in the throttle angle. Its profile shows the desired characteristics of the intake manifold pressure in response to a sudden change in the throttle angle, as well as returning to the same steady state condition after the throttle angle has been returned to its original position. The magnitude of the pressure also supports the validity of this model since it is less than atmospheric pressure and is at a level that is appropriate for an engine of this type.

In the four to six second range of the simulation, the intake manifold pressure shows some signs of instability. This is characterized by the wavering pressure trace through this time period. The throttle body and intake manifold models cause the instability, which is due to the non-linear, non-choked flow equation of the intake manifold, the air momentum effects in the intake manifold and the reverse-looking predictive model. Using a more realistic air momentum model could eliminate most of this problem. Currently a moving average of the intake manifold pressure is used to account for air momentum effects. Little research has been completed on this aspect of the model development. The present condition of the model has proved to be robust in all other conditions, and this slight fluctuation only appears at large (>30°) throttle angles.

The power output increases proportionally as the engine speeds up (see Fig. 3.1). This is expected with the constant load that is applied and the constant throttle position after the step increase. After the throttle is stepped back down to its original position, there is a sharp drop off in power output. This is expected since the power output shown in Fig. 3.1 is calculated based on the work of the expanding air/fuel mixture in the combustion chamber. The information displayed in Fig. 3.1 does not account for the power output of the energy stored in the rotating inertia of the engine. For the purpose of a complete APU model, the power output should be calculated directly from the speed of the engine and the torque applied to it. For validation purposes, the power output from pressure work is more useful because it shows what is happening in the combustion equations of the engine model.

2.7.3 Closed Loop Engine Speed Control

Closed loop speed control of the IC engine model is accomplished by using the *control.m* function inside of the model loop inside of *run_sim.m*. *Control.m* is a proportional and derivative (PD) control algorithm that compares the current speed of the IC engine model with a desired engine speed set point that is entered in *run_sim.m.* A PD speed control of the IC engine is attractive because it is easy to obtain the hardware for implementation, it is inexpensive and the methods for setting up a PD and PID controller are well known.

Two test cases are shown in Fig. 3.2 and 3.3. These simulations use closed loop speed control of the same Yamaha engine listed in Table 3.1 under a step disturbance of the load torque and a ramp disturbance of the load torque. Step and ramp disturbances are commonly used to evaluate the performance of a controller, which is one of the purposes for showing both of these test cases. The other purpose for showing step and ramp disturbances is that they are they also represent possible real operating conditions of an APU operating in a series HEV.

Batteries with a low SOC have a reduced power density. This means that they are not capable of sustaining high power demands. After the batteries are producing as much power as can, the alternator must make up the rest of the required power. A full throttle step input to the propulsion system will result in a near step response in the load applied to the engine in this situation. Figure 3.2 shows the engine and control system reaction to a step change in the torque applied to the IC engine.

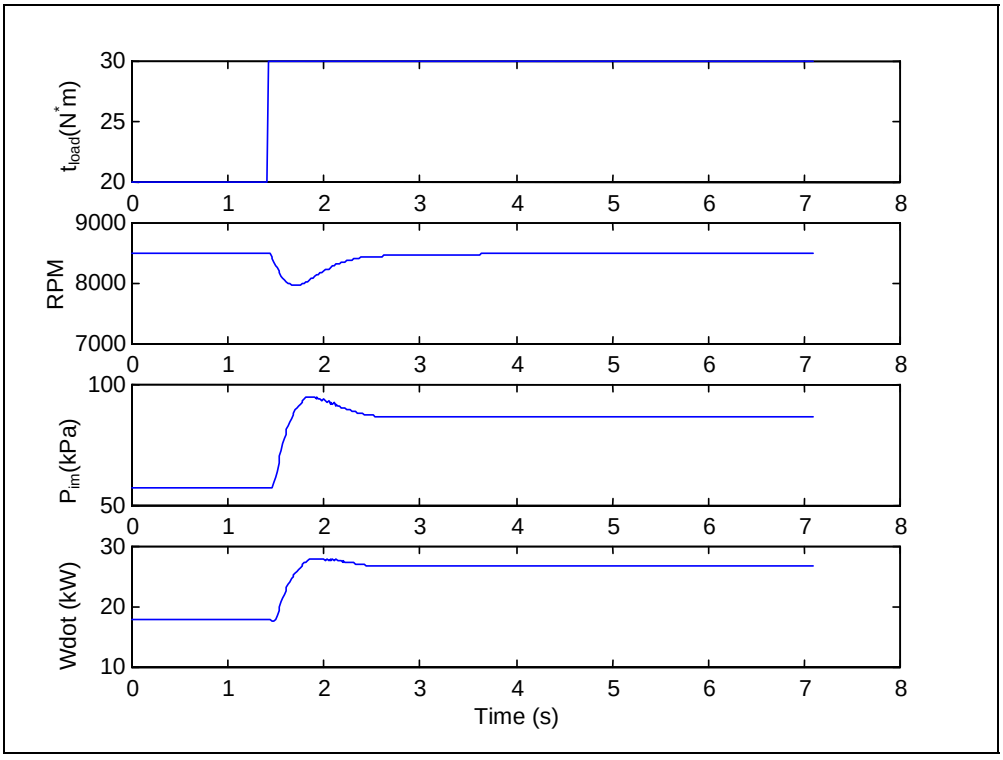

Figure 3.2 Closed loop speed control with step disturbance

When there is a high power demand from the vehicle propulsion system at higher battery pack charge levels, the battery pack is more capable of delivering the required power. This will result in delayed ramp loading on the engine. A ramped torque load on the engine is shown in Fig. 3.3. At lower states of charge, a high power demand from the propulsion system will have a different effect on the alternator load and therefore, the load seen by the IC engine.

The control constants used in the closed loop simulations shown in Fig. 3.2 and Fig. 3.3 were both the same at K_p = .000008 and K_D = .000008. These values are small because the closed loop control output is in units of radians, which has very small numeric inputs to the IC engine model. This must be changed when a known controller is used. Most likely its inputs will be a voltage or current from a sensor, and the output will likewise be a voltage or current sent to an actuator.

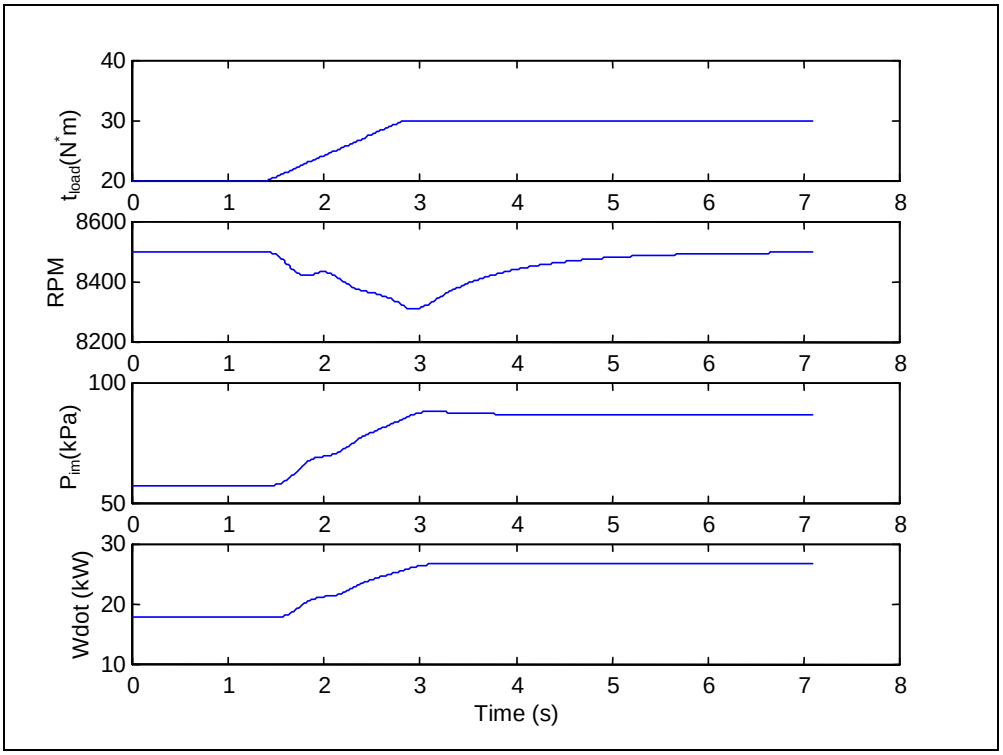

Figure 3.3 Closed loop speed control with ramp disturbance

These two test cases help show the robustness of this model and the ability of a PD control to provide reasonable control. The performance of this system could be improved with further optimization of the controller constants and adding integral control. There has not been extensive work put into the optimization of the controller constants used for the test cases presented.

2.7.4 Load Control Strategy

Engine fuel efficiency is dependent upon the load seen by the engine and the speed of operation. The most efficient engine operation occurs over a very narrow range of RPM and a slightly larger range of load. To be able to relate the amount of divergence from the RPM set point to the effect on the overall efficiency, a fuel map of the engine is needed. In general, a divergence of less than 100 RPM has no effect on the overall efficiency. In both cases above, a divergence from the set RPM occurs by more than 100 RPM. This means there is room for improvement of this controller and possibly of the speed control strategy.

Another strategy to consider is that of load and speed control. Load control could be accomplished by using a field-controlled alternator. With a properly designed control system, the load experienced by the engine would be nearly constant. Speed control would only be necessary for startup and shutdown of the engine and error handling ability, in the event of a high voltage system or alternator control failure. A field-controlled alternator would also eliminate the problems associated with the non-linear load transition of fixed field alternators. The disadvantage to a field-controlled alternator is the added power electronics and a slightly more complex system. These disadvantages may be outweighed by improved fuel efficiency and reduced emissions.

3.0 Conclusion

Using the steady state road load model, a series HEV was designed to operate mostly as a zero tailpipe emission electric vehicle that uses commercially available starved electrolyte lead-acid batteries for energy storage. This series HEV also has an extended range capability of 400 miles using a small, high-speed, gasoline/electric auxiliary power unit and a zero emission range of 60 miles at 55 mph using stored energy from the grid. The end result is a vehicle with

performance that is comparable to conventional production vehicles in extended range situations, but operates as a zero emission electric vehicle for most everyday driving situations. Having an APU that is high powered (>20kW), small and low weight is the key to making this system feasible.

A high performance APU that provides 20 to 30 kW (25 to 40 hp) of continuous power while weighing approximately 90 pounds and taking up about three cubic feet of space, not including the exhaust and cooling systems, can be realized using commercial components. This HPAPU consists of a Yamaha 250cc, four-stroke SI engine and a Fisher permanent magnet alternator operating at a minimum of 6000 RPM. By operating at a high speed, this Fisher alternator can produce the same power as one that is much larger and heavier. Although this HPAPU provides good performance with off-the-shelf components, further volume and weight reductions would be possible with specially developed engines and alternators.

A model for characterizing a series HEV under steady state conditions has been developed. This model determines the steady state road load for the entire vehicle and helps to size the required battery pack to meet a given range requirement. Knowing the required road load allows the designer to appropriately size the engine and alternator for a high performance APU. The steady state road load model was used to study the impacts of an improved lead-acid battery pack on the performance of a series HEV. Commercially available 35 W*hr/kg starved electrolyte lead-acid batteries were used as a baseline and then compared to an improved starved electrolyte lead-acid battery design that uses paste additives with a specific energy of 55 W*hr/kg. The results of this study found the improved lead-acid battery design would reduce the vehicle weight by 355 pounds, reduce the size of the battery pack by 2.5 cubic feet and improve the steady state highway fuel economy by approximately 5 percent at a speed of 55 mph. The reduction of the vehicle weight has little effect on the steady state HPAPU power requirement.

An IC engine model was developed to dynamically simulate small engines and assist in the design of series HEVs. The engine model was validated at a single point against a Yamaha

YZ250N 4-stroke engine. Factory specifications for this engine claimed a power output of 30.5 kW at 8500 RPM, and the engine model returned a power output of 30.8 kW at 8561 RPM. Inspecting the response of RPM, intake manifold pressure and power output has also validated the behavior of this engine model to a step change in throttle position while constant torque was applied. A closed loop, proportional/derivative, speed control system was implemented with the dynamic engine model and proved to be robust, which is an important step towards the development of a complete HPAPU dynamic model.

3.1 Recommendations

The engine model still needs to be validated over the entire speed and loading range. The results of this validation would show whether or not cylinder heat loss, engine friction, pumping work, and possibly an improved intake manifold model should be included in the model or if the volumetric efficiency term would suffice for application as a control system development model. The next step to building a complete dynamic HEV simulation tool is adding alternator and battery models. Having these steps completed would allow the development of APU control strategies that are optimized for the best possible efficiency during a standardized federal driving cycle test.

With a moderate amount of work, the engine model could be modified to include emission estimates. Including engine friction, heat transfer through the cylinder walls and a real fuel delivery model will be required. More research is required to determine if the addition of dynamic emission estimates would be more beneficial than using steady state engine emission maps.

If an engine were designed specifically for the application of a HPAPU, a two-stroke spark ignition gasoline engine would be ideal. Two-stroke engines are viewed as simple, lightweight, high powered, noisy, inefficient and dirty in terms of emissions. This is all true for the current applications of two-stroke engines. Two-stroke engines are used when low weight and high power is desired and fuel efficiency and emissions are not a factor. As an APU power source,

the two-stroke engine provides the advantage of low weight and high power output in an environment where the fuel efficiency and emissions output problems can be avoided.

With a speed- and or load-controlled system, the engine can run at a relatively constant speed. This would allow a tuned pipe to provide nearly perfect scavenging efficiency, which would lead to much lower emissions and higher fuel economy from a two-stroke engine. In addition, some space and weight could be sacrificed to include a lubrication system for the engine, thereby eliminating the need for oil mixed in the fuel and the emissions associated with it.

For short-term bench testing and in vehicle prototyping, a microcontroller, programmable logic controller (PLC) or an industrial computer will be sufficient. For extended testing, a dedicated automotive vehicle controller will be required. Automotive style vehicle controllers are available that can be programmed with conventional personal computers.

APPENDIX I: NOMENCLATURE

a = Weibe function constant

A_p = area of piston

APU = auxiliary power unit

A_{th} = open throttle area

A_F = frontal area of vehicle

(A/F) = air fuel ratio

$(A/F)_s$ = stoichiometric air fuel ratio

C_D = discharge coefficient

CD = drag coefficient

C_R = rolling resistance coefficient

CR = compression ratio

d_i = throttle plate shaft diameter

dt = time step

HEV = hybrid electric vehicle

HPAPU = high performance auxiliary power unit

IC = internal combustion

L_{cr} = connecting rod length

L_{ct} = crank shaft radius

LHV = lower heating value

m = Weibe function constant

m_{im} = mass of air in intake manifold

m_{fuel} = mass of fuel in cylinder

$\dot{m}_{cyl}$ = mass flow rate into cylinder

$\dot{m}_{th}$ = mass flow rate past throttle

n = number of cylinders

nr = number of rev / power cycle

T_{im} = intake manifold air temp.

T_o = ambient air temp. (absolute)

p = pressure

PD = proportional/derivative

PID = proportional/integral/derivative

p_{im} = intake manifold pressure (absolute)

p_o = ambient pressure (absolute)

P_r = required horsepower

Q_h = fuel entropy

R = universal gas constant

R_{air} = ideal gas constant for air

RPM = rotations per minute

RPM* = rotations per minute set point

SI = spark ignition

SOC = state of charge

V = volume of cylinder

V_{cv} = clearance volume

V_{ic} = volume in cylinder at intake close

V_{MPH} = vehicle velocity (MPH)

V_{sv} = swept volume

x_B = mass burn fraction (Weibe)

$\dot{W}_{ave}$ = average power output

W_V = vehicle weight (lbs)

ZEV = zero tailpipe emission vehicle

α = throttle plate angle

α_c = throttle plate angle at close

γ = specific heat ratio

η_v = volumetric efficiency

λ = equivalence ratio

ρ_{im} = intake manifold density

ρ_{fi} = intake fuel density

θ = crank angle

θ_o = ignition timing

$\Delta\theta$ = burn duration angle

τ_{engine} = average torque output

τ_{load} = load torque on engine

$\tau_{net} = \tau_{engine} - \tau_{load}$

REFERENCES

[1] Hu, P.S., and J. R. Young, *Summary of Travel Trends 1995 Nationwide Personal Transportation Survey*. US DOT Federal Highway Administration, December 1999.

[2] Davis, S. C., *Transportation Energy Data Book.* Ed. 20. Oak Ridge National Laboratory Oak Ridge, Tennessee, November 2000.

[3] *Household Vehicles Energy Consumption 1994 - Appendix B,* http://www.eia.doe.gov/emeu/rtecs/appendb2.html, April 2001.

[4] United States Department of Energy, SCNG—Project Data, *High Efficiency Fossil Power Plants (HEFPP) Conceptualization Program DE-RA26-97FT34164* http://www.netl.doe.gov/

[5] Heywood, J. B., *Internal Combustion Engine Fundamentals*. New York: McGraw-Hill, Inc., 1988.

[6] *Motortrend Online Buyer's Guide*, www.motortrend.com, April 2001.

[7] *AC Propulsion AC 150 Specifications*, factory supplied information, April 2001.

[8] Cantrell, R. L., *Modeling and Designing a High Performance Lead-Acid Battery for Hybrid Electric Vehicles*. Masters Thesis, University of Idaho, 1996.

[9] Dayton, T. B., and D. B. Edwards, "Improving the Performance of a High Power, Lead-Acid Battery with Paste Additives," *Journal of Power Sources* 85 (2000), pp. 137-144.

[10] Edwards, D.B., "An Electric Vehicle Design Based on a High-Power, Sealed, Lead-Acid Battery," Society of Automotive Engineers #881790, 1988.

[11] Taylor, C. F., *The Internal Combustion Engine in Theory and Practice.* Vol. 1. 2nd Ed. Cambridge, MA: MIT Press, 1985.

[12] www.honda2001.com/models/civic_coupe/features.html, April 2001.

[13] Blair, G. P. *Design and Simulation of Four-Stroke Engines*. Warrendale, PA: Society of Automotive Engineers, 1999.

[14] Blair, G. P., *Design and Simulation of Two-Stroke Engines*. Warrendale, PA: Society of Automotive Engineers, 1996.

[15 Kinsler, L. E., et. al., *Fundamentals of Acoustics.* 4th Ed. New York: John Wiley & Sons, 2000.

[16] Yamaha Motor Corp., Factory Provided Information, April 2001.

[17] Fisher Electric Technology, Inc., Factory Provided Information, February 2001.

[18] Moran, M. J., *Fundamentals of Engineering Thermodynamics*. 3rd Ed. New York: John Wiley & Sons, 1995.

[19] Heywood, J. B., J. M. Higgins, P. A. Watts and R. J. Tabaczynski, "*Development and Use of a Cycle Simulation to Predict SI Engine Efficiency and NO_x Emissions*," Society of Automotive Engineers #790291, 1979.

[20] Reiche, D. B. *Simulating Standard and Local Driving Cycle Performance of a Series Hybrid Electric Vehicle*. Master's Thesis, University of Idaho, September 2000.